



## Greatly enhanced fluorescence of dicyanamide anion based ionic liquids confined into mesoporous silica gel

Juan Zhang<sup>a,b</sup>, Qinghua Zhang<sup>a,b</sup>, Feng Shi<sup>a,b</sup>, Shiguo Zhang<sup>a,b</sup>, Botao Qiao<sup>a</sup>, Lequan Liu<sup>a,b</sup>, Yubo Ma<sup>a,b</sup>, Youquan Deng<sup>a,\*</sup>

<sup>a</sup> Centre for Green Chemistry and Catalysis, Lanzhou Institute of Chemical Physics, Chinese Academy of Sciences, Lanzhou, China

<sup>b</sup> Graduate University of the Chinese Academy of Sciences, Beijing, China

### ARTICLE INFO

#### Article history:

Received 21 April 2008

In final form 3 July 2008

Available online 9 July 2008

### ABSTRACT

1-Ethyl-3-methylimidazolium dicyanamide EMImN(CN)<sub>2</sub> and S-ethyltetrahydrothiophene dicyanamide ETN(CN)<sub>2</sub> physically confined into mesoporous silica gel with pore sizes of 6–8 nm (IL-sg) were synthesized according to a proper sol–gel process. Greatly enhanced fluorescence emissions of dicyanamide based ILs after being confined were exhibited.

© 2008 Elsevier B.V. All rights reserved.

### 1. Introduction

Nano-technology has been the subject of enormous interests in the past decade because of their potential and wide-ranging industrial, chemical, biomedical, and electronic applications [1–5]. As a bridge between single molecules and infinite bulk systems, the chemical and physical properties of nano-materials could significantly differ from those of the atomic-molecular and bulk materials of the same chemical composition and offers significant potentials in building new types of devices with atomic or molecular precision [6]. In previous studies, nano-materials concerned were basically metals, ceramics, polymeric materials, or composite materials, i.e. they are all solids in macroscopic scale. Reports on liquids confined in various nano-scale matrices, which may also exhibit different or novel physicochemical properties [7–14] in comparison with the bulk fluids or liquids, however, are still scarce probably due to the difficulties in obtaining ‘nano-liquid particles’ with enough stability or in characterizing experimentally.

Though not new, room temperature ionic liquids (ILs) have attracted much attention due to their potential applications as novel media and soft materials in both academia and industry fields [15–17]. The ILs properties such as negligible vapor pressure, low melting points and high thermal stability make it possible to prepare confined ILs within nano-scale matrices and peculiar properties may exhibit. For example, it has been reported that abnormal Raman spectra of nano-confined 1-butyl-3-methylimidazolium tetrafluoroborate BMImBF<sub>4</sub> in mesoporous silica gel with pore size smaller than 11 nm compared with bulk IL were observed [18].

The liquid properties can be controlled in combination with nanoporous silica glass and melting point of RTILs showed a remarkable decrease in proportion to inverse of pore size [19]. BMImPF<sub>6</sub> confined into multiwalled carbon nanotubes exhibited phase transition, liquid-like behavior at temperatures below the crystallization temperature of the original IL [20]. 2D correlation spectra showed ILs conformational changes in ILs-aluminum hydroxide hybrids [21]. Vioux et al. have used sol–gel method to synthesize a series of ionogel materials with confinement of ILs into open mesoporous oxide networks and the ionic liquids dynamics confined in monolith silica matrices were studied [22–27]. Computer simulations of the structure and dynamics of 1,3-dimethylimidazolium chloride confined between two parallel structureless walls showed that ionic diffusion was faster than in the bulk ILs [28]. The solvent and rotational relaxation of C-153 in BmimBF<sub>4</sub> confined alkyl poly(oxyethyleneglycol) containing micelles suggested a slight decrease in the solvation time compared to that of bulk BmimBF<sub>4</sub> [29]. And more recently, near-spherical solid-state (frozen) IL nanoparticles were successfully synthesized based on a novel melt–emulsion–quench approach and novel properties may exhibit [30]. As we know, most of ILs reported are found to be fluorescent [31–33], however, possible effect of their confinement into nano-scale matrices on the photoluminescence properties of ILs has not been studied yet.

In this work, ILs with dicyanamide anion confined within mesoporous silica gel were synthesized according to ‘one-pot assembly’ of ILs and silicate ester through a proper sol–gel process. It should be emphasized that the key concept of designing and synthesizing such nano-confined ILs involves the physical confinement of hydrophilic RTILs. Then the fluorescence emissions and the reasons for the emissions of confined dicyanamide anion based ILs within mesoporous silica gel were discussed in comparison with pure ILs.

\* Corresponding author. Fax: +86 931 4968116.

E-mail address: [ydeng@lzb.ac.cn](mailto:ydeng@lzb.ac.cn) (Y. Deng).

## 2. Experimental

### 2.1. Materials

All chemicals used in the experiments were of analytical grade, and were used without further purification. Silver dicyanamide  $\text{AgN}(\text{CN})_2$  was purchased from Aldrich and used as received.

### 2.2. Synthesis of ILs, mesoporous silica gel confined $\text{EMImN}(\text{CN})_2$ , $\text{EMImBF}_4$ and $\text{EThN}(\text{CN})_2$ denoted as IL-sg

ILs used in this work were synthesized carefully and purified rigorously in our laboratory. The process was described in the [Supplementary material](#).  $\text{EMImN}(\text{CN})_2$  (0.05–1.0 g) was dissolved

into the solution of tetraethyl orthosilicate (5.00 mL) and ethanol (2.50 mL) and was stirred for 2 h under 40 °C. Then the solution was cooled to room temperature into which 2.50 mL hydrochloride aqueous solution (mixture of 10.00 mL distilled water and 0.02 mL 37% concentrated hydrochloride acid) was added dropwise under vigorous stirring. After 5 h, the solution was exposed to vacuum at 60 °C for 2 h for the removal of the ethanol solvent during which a transparent gel was formed. And then after the gel was aged for 24 h in the air at 60 °C, the obtained materials with different loading of  $\text{EMImN}(\text{CN})_2$  in mass were subjected to a higher vacuum at 100 °C for 5 h to eliminate the volatile components for the immediate fluorescence characterization. IL-sg involving  $\text{EMImBF}_4$ ,  $\text{EThN}(\text{CN})_2$  were synthesized according to the same procedure. The loadings of ILs were calculated through the ratio of the mass

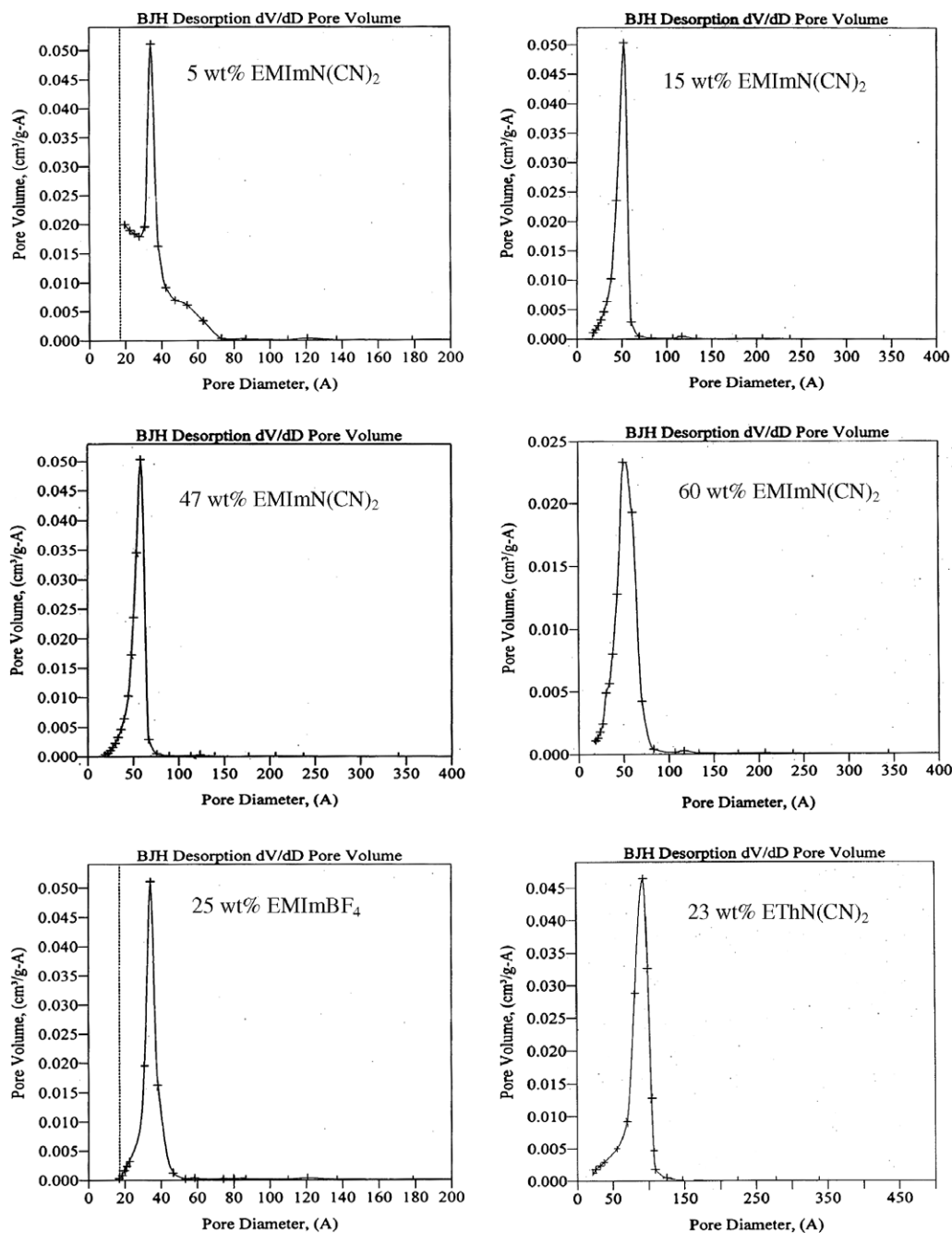


Fig. 1. BET pore size distribution plots of wsg-IL with ILs  $\text{EMImN}(\text{CN})_2$ ,  $\text{EThN}(\text{CN})_2$  and  $\text{EMImBF}_4$ .

of the ILs initially involved to the total amount of IL-sg material finally obtained.

### 2.3. Preparation of silica gel by drastic washing of ILs from IL-sg, denoted as wsg-IL

IL-sg was washed with mixture of ethanol and acetone (v/v, 1:1) under refluxing at 60 °C for 12 h and this procedure was repeated for three times for the drastic washing of IL, and then was filtrated. The solid of silica gel was treated at 100 °C under vacuum for 24 h to eliminate volatile phase remained in the material.

### 2.4. Characterizations and instruments

N<sub>2</sub> adsorption measurements were obtained using a Micromeritics ASAP 2010 instrument to measure the surface area and porosity of wsg-IL using nitrogen at 77 K as the standard adsorptive gas. The surface area was obtained by the Brunauer–Emmett–Teller (BET) method and the pore size distribution was calculated from the adsorption branch of the isotherm using the Barrett–Joyner–Halenda (BJH) method. The thermal decomposition temperatures and weight loss were assessed by employing a Pyris Diamond TG/DTA analyzer at a heating rate of 10 °C/min under nitrogen atmosphere. UV spectra were conducted on an Agilent 8453 UV-vis spectrophotometer. The fluorescence spectra were recorded at 25 °C on a Hitachi model F-7500 FL spectrophotometer (Hitachi, Japan) with a xenon lamp as the excitation source. The excitation and emission slit widths were 2.5 and 1.0 nm, respectively. The photomultiplier voltage was 700 V. FT-IR spectra were recorded on a Thermo Nicolet 5700 FT-IR spectrophotometer. FT-Raman characterization was carried out over a Nicolet 950 laser Raman spectroscopy.

## 3. Results and discussion

BET results of wsg-EMImN(CN)<sub>2</sub> with varied IL loadings (Fig. 1, Table 1 and Fig. S1 in Fig. S1 in Supplementary material) showed that, wsg-EMImN(CN)<sub>2</sub> had the characteristic absorption isotherm type of mesoporous materials. With EMImN(CN)<sub>2</sub> loading of 5 wt%, the average pore diameter of wsg-EMImN(CN)<sub>2</sub> is 5.6 nm. When the loading is increased to 15 wt%, the average pore diameter of wsg-EMImN(CN)<sub>2</sub> is increased to 7.6 nm. When IL loading was further increased to be 24 and 47 wt%, the average pore diameter was 7.9–7.7 nm, respectively, suggesting that the average pore diameter was not changed anymore with further increasing of IL loading higher than 15 wt%. It may be suggested that, with EMImN(CN)<sub>2</sub> loading higher than 15 wt%, with the in variation of the pore sizes of wsg-EMImN(CN)<sub>2</sub>, the extra part of EMImN(CN)<sub>2</sub> may be gradually aggregated on the external surface of the support. It is also shown that, EMImN(CN)<sub>2</sub>-sg with EMImN(CN)<sub>2</sub> loading from 15

to 60 wt% had a narrow pore size distribution range. BET results (Table 1) showed that, with IL loading increasing from 5 to 23 wt% and further to 60%, average pore diameter of wsg-ETHN(CN)<sub>2</sub> was increased from 3.5 to 6.9 nm and then no changes in the sizes of nanopores of wsg-ETHN(CN)<sub>2</sub> can be observed, which was similar to the BET measurements of wsg-EMImN(CN)<sub>2</sub> in general trend. And the average pore diameter of wsg-EMImBF<sub>4</sub> with EMImBF<sub>4</sub> loading of 25 wt% was 5.5 nm. These results can also suggest that the sizes of the pore diameter of wsg-IL could be slightly adjusted by the variations of IL itself.

Pure EMImN(CN)<sub>2</sub> and ETHN(CN)<sub>2</sub> (Fig. S2) showed the similar absorption spectra in shape and nature. Compared with pure EMImBF<sub>4</sub> whose absorption spectrum is consistent with previous reports [31], pure EMImN(CN)<sub>2</sub> and ETHN(CN)<sub>2</sub> display obvious absorption above 300 nm, assigned to the  $\pi$ - $\pi^*$  electron transition due to the presence of  $\pi$  delocalized electrons in the dicyanamide anion.

The fluorescence emission spectra of pure EMImN(CN)<sub>2</sub>, 15 wt% EMImN(CN)<sub>2</sub>-sg and the corresponding wsg-EMImN(CN)<sub>2</sub> were comparatively measured, in Fig. 2 and Fig. S3. Pure EMImN(CN)<sub>2</sub> (Fig. 2a) was found to be fluorescent with excitation wavelength  $\lambda_{ex}$  from 320 to 440 nm. The emission band  $\lambda_{em}$  exhibited a remarkable shift from 386 to 491 nm with  $\lambda_{ex}$  from 320 to 440 nm. And fluorescence emission of pure EMImN(CN)<sub>2</sub> was strongly dependent on the excitation wavelength, and a long absorption tail and shifting nature similar to that reported before [33] can be observed probably due to the presence of various association forms in the pure IL. When excited at 360 nm, its emission maximum  $\lambda_{max}$  was observed at 424 nm, and it can be seen that the intensity of pure EMImN(CN)<sub>2</sub> was comparatively weak. In comparison with pure EMImN(CN)<sub>2</sub>, EMImN(CN)<sub>2</sub>-sg (Fig. 2b) exhibited notably different fluorescence with excitation range 240–380 nm, and  $\lambda_{max}$  was observed at 370 nm with excitation of 300 nm, i.e. fluorescence occurred at a relatively lower wavelength and  $\lambda_{max}$  was decreased by 56 nm after being confined. Moreover, the emission band of EMImN(CN)<sub>2</sub>-sg was independent on the excitation when  $\lambda_{ex}$  was lower than 320 nm. This is very different compared with the emission tail nature and strong excitation-dependent fluorescence emissions of pure IL [33]. With  $\lambda_{ex}$  of 360 nm, the emission band of EMImN(CN)<sub>2</sub>-sg showed a remarkable red shift to 399 nm. Especially, compared with pure EMImN(CN)<sub>2</sub>, greatly enhanced fluorescence of confined EMImN(CN)<sub>2</sub> appeared, e.g. the emission intensity of 15 wt% EMImN(CN)<sub>2</sub>-sg was about 100 times stronger than that of pure EMImN(CN)<sub>2</sub>. However, the obvious fluorescence of wsg-EMImN(CN)<sub>2</sub> could be still observed, although it displayed weaker emission intensity than the material before washing. This indicates that there might be some EMImN(CN)<sub>2</sub> remained in wsg-EMImN(CN)<sub>2</sub>. Therefore, the fluorescence emission of pure silica gel without any employed IL was then measured (Fig. S3d). It is shown that, pure silica gel almost did not display any obvious emissions in the range of 350–450 nm with varied  $\lambda_{ex}$ . So it indicates that, the stronger fluorescence emissions of EMImN(CN)<sub>2</sub>-sg are resulted from EMImN(CN)<sub>2</sub> confined in the materials. After drastic washing of EMImN(CN)<sub>2</sub>-sg, the content of the remained EMImN(CN)<sub>2</sub> measured by TG/DTA results was ca. 0.6 wt% (Fig. S3e), which resulted in the obvious emissions of wsg-EMImN(CN)<sub>2</sub>. However, the emission of wsg-EMImN(CN)<sub>2</sub> is more irregular in the spectra shape, so there are not more discussions on this issue herein.

Possible contributions of cation and anion moiety to the strong fluorescence emission of IL-sg based on dicyanamide ILs were further tested. When N(CN)<sub>2</sub> was replaced with BF<sub>4</sub><sup>-</sup>, the fluorescence of pure EMImBF<sub>4</sub> and EMImBF<sub>4</sub>-sg were measured (Fig. S4). Pure EMImBF<sub>4</sub> (Fig. S4a) was found to be fluorescent with excitation from 280 to 400 nm, and  $\lambda_{max}$  = 412 nm when being excited at

**Table 1**  
BET characterizations of wsg-IL

RTIL	IL loading (wt%)	Average pore diameter (nm)	BET surface area (m <sup>2</sup> /g)	Total pore volume (cm <sup>3</sup> /g)
EMImN(CN) <sub>2</sub>	5	5.6	444	0.75
	15	7.6	390	0.86
	24	7.9	386	0.72
	47	7.7	386	0.76
	60	7.9	383	0.78
ETHN(CN) <sub>2</sub>	5	3.5	586	0.56
	17	6.5	420	0.71
	23	6.9	416	0.79
EMImBF <sub>4</sub>	40	6.8	422	0.73
	60	6.8	420	0.76
	25	5.5	451	0.72

300 nm, i.e. excitation occurred at relatively lower wavelength after  $N(CN)_2^-$  was replaced with  $BF_4^-$ , and the fluorescence intensity was comparable to that of pure  $EMImN(CN)_2$ . After being confined (Fig. S4b),  $EMImBF_4$ -sg showed irregular emission band at 300–450 nm which is very similar to pure silica gel, and its fluorescence intensity was still very weak, i.e. unlike  $EMImN(CN)_2$ ,  $EMImBF_4$  did not exhibit enhanced fluorescence emission after being confined into the mesoporous silica gel Fig. 3.

When  $EMIm$  cation was changed with *S*-ethyltetrahydrothiophene (ETH), pure  $ETHN(CN)_2$  (Fig. 4a) showed a shifting nature of fluorescence emission from 396 to 496 nm with excitation 340–460 nm and  $\lambda_{max} = 439$  nm with excitation of 380 nm, i.e. fluorescence occurred at a relatively higher excitation wavelength after  $EMIm$  was replaced with ETH cation, and the fluorescence intensity was slightly weaker than that of pure  $EMImN(CN)_2$ . After being confined, a typical result (Fig. 5b) showed that the fluorescence

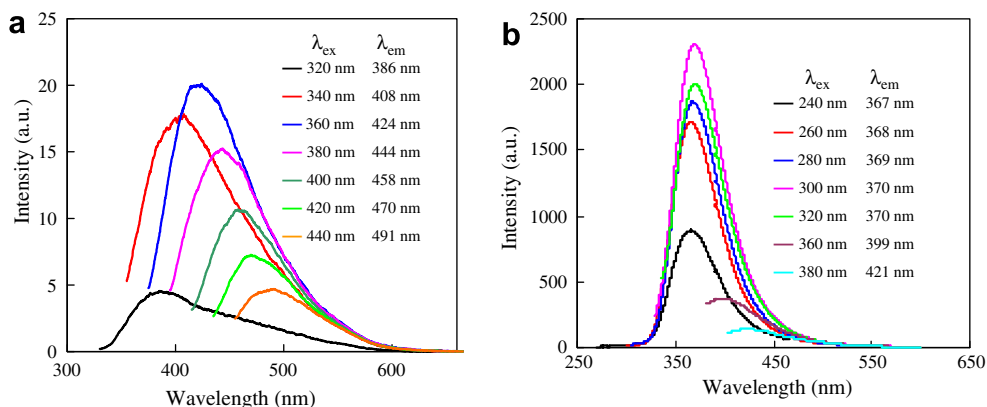


Fig. 2. Emission behavior of (a) bulk  $EMImN(CN)_2$  and (b)  $EMImN(CN)_2$ -sg (15 wt%) with varied excitation wavelength ( $\lambda_{ex}$ ).

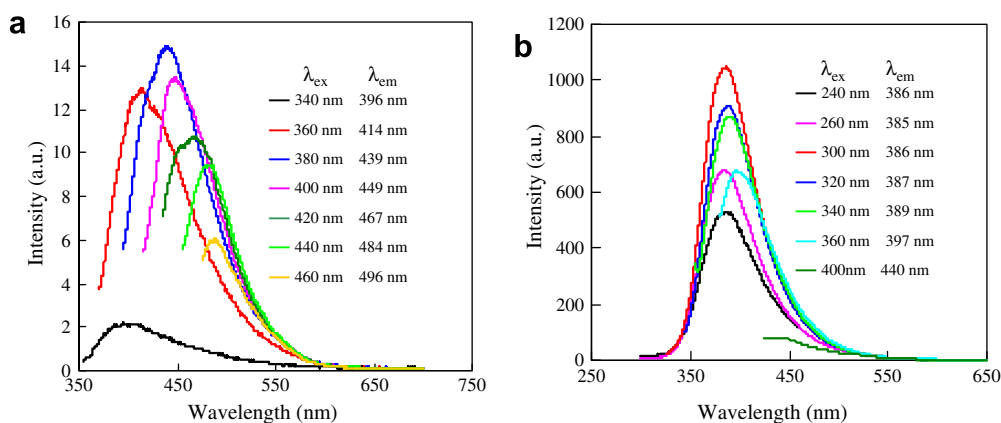


Fig. 3. Emission behavior of (a) bulk  $ETHN(CN)_2$  and (b)  $ETHN(CN)_2$ -sg (23 wt%) with excitation wavelength ( $\lambda_{ex}$ ).

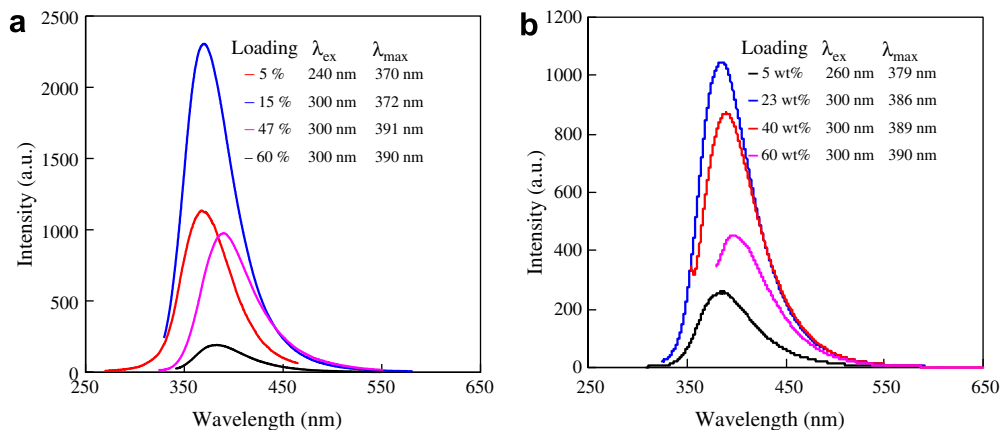


Fig. 4. Emission maximum of (a)  $EMImN(CN)_2$ -sg, and (b)  $ETHN(CN)_2$ -sg with varied IL loadings.

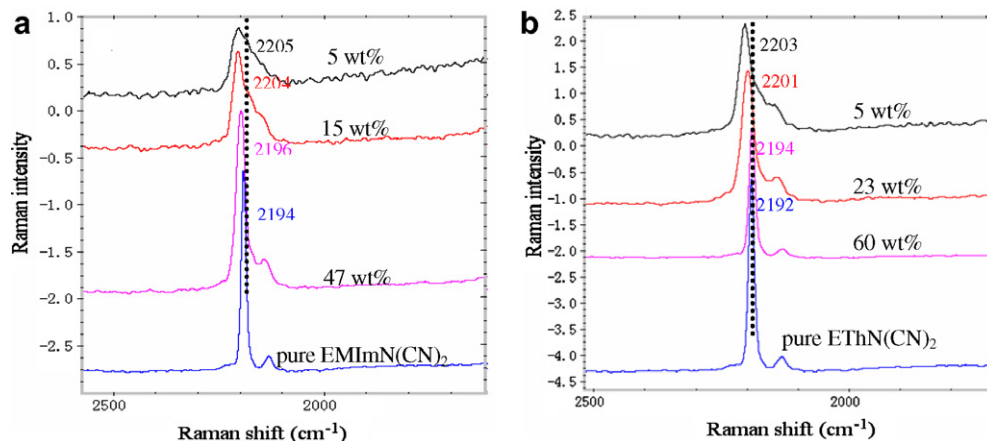


Fig. 5. FT-Raman spectra of (a) EMImN(CN)<sub>2</sub>-sg and (b) EThN(CN)<sub>2</sub>-sg with varied IL loadings.

emission of EThN(CN)<sub>2</sub>-sg with 23 wt% EThN(CN)<sub>2</sub> loading was observed with excitation wavelength from 240 to 400 nm and fluorescence emission maximum  $\lambda_{\text{max}} = 386$  nm with  $\lambda_{\text{ex}}$  of 300 nm, *i.e.* fluorescence emission maximum was observed at a relatively lower wavelength and the  $\lambda_{\text{max}}$  was decreased by 53 nm after being confined, which was similar to that of confined EMImN(CN)<sub>2</sub> in general trend. Moreover, the emission band of EMImN(CN)<sub>2</sub>-sg was independent on the excitation with  $\lambda_{\text{ex}}$  lower than 360 nm, and greatly enhanced fluorescence was also observed, *i.e.* the intensity of EThN(CN)<sub>2</sub>-sg with IL loading 23 wt% was about 70 times as that of pure EThN(CN)<sub>2</sub>.

Based on the experimental results and the fact that, *i.e.* as observed in Fig. 2a and Fig. S4a, pure EMImN(CN)<sub>2</sub> showed an excitation-dependent emission, and EThN(CN)<sub>2</sub> displayed a similar fluorescence to EMImN(CN)<sub>2</sub>. Previous studies on the fluorescence emissions of some 1,3-dialkylimidazolium salts [31–33] suggests that, the various associations from the  $\pi$  stackings of imidazolium cations may lead to the excitation-dependent emissions of pure ILs. As for IL with N(CN)<sub>2</sub><sup>-</sup> as anion, after the replacement of EMIm by ETh with the absence of  $\pi$  electrons in the cation, the obvious fluorescence emissions of EThN(CN)<sub>2</sub> similar to EMImN(CN)<sub>2</sub> could be also observed. So in this case, the presence of the N(CN)<sub>2</sub><sup>-</sup> anion could make important contribution to the fluorescence emission of dicyanamide based ILs.

Then, the fluorescence of EMImN(CN)<sub>2</sub>-sg with varied loading from 5 to 60 wt% was studied and compared (Fig. 4 and Fig. S6).  $\lambda_{\text{max}}$  varied from 370 ( $\lambda_{\text{ex}}$ : 260 nm) to 390 nm ( $\lambda_{\text{ex}}$ : 320 nm) correspondingly, *i.e.* a red shift occurred monotonously with increase of EMImN(CN)<sub>2</sub> loadings. However, the emission intensity was initially increased, reached to maximum at 15 wt%, and then decreased quickly with further increasing of EMImN(CN)<sub>2</sub> loading. It can be seen that the EMImN(CN)<sub>2</sub>-sg with IL loading 15 wt% and 7.6 nm of pore size of wsg-EMImN(CN)<sub>2</sub> exhibited the strongest fluorescence emission (Fig. 4a). With loading being increased, a notable decrease in fluorescence emission intensity was observed. As indicated that the pore diameter was almost not changed when IL loading was increased from 15 wt% to the higher, the increased IL may aggregate on the external surface of silica gel, therefore, it resulted in the decrease of the emission intensity. However, the emission intensity of EMImN(CN)<sub>2</sub>-sg with IL loading 5 wt% and 5.6 nm of average pore diameter of wsg-EMImN(CN)<sub>2</sub> was slightly higher than that with 47 wt% of loading and 7.7 nm of average pore diameter as shown in Fig. 4a. These results suggested that, the intensity of fluorescence emission of EMImN(CN)<sub>2</sub>-sg was largely dependent on the loading of EMImN(CN)<sub>2</sub> in the silica gel. EMImN(CN)<sub>2</sub> confined in the pores

with 7–8 nm in size and 15 wt% of IL loading exhibited the strongest fluorescence emission.

As for EThN(CN)<sub>2</sub>-sg with different IL loadings (Fig. 4b and Fig. S7), similar results as EMImN(CN)<sub>2</sub>-sg can be obtained. With EThN(CN)<sub>2</sub> loading 5 wt%,  $\lambda_{\text{max}}$  was observed at 379 nm with excitation 260 nm, and when increased to 23 wt%,  $\lambda_{\text{max}} = 386$  nm with excitation 300 nm,  $\lambda_{\text{max}}$  and  $\lambda_{\text{ex}}$  were both increased to a higher wavelength. Meanwhile, the fluorescence emission intensity was remarkably increased to the strongest among the EThN(CN)<sub>2</sub>-sg with varied IL loadings. With further increasing of EThN(CN)<sub>2</sub> loading from 23 wt% to the higher, it showed a monotonous red shift of emission maximum  $\lambda_{\text{max}}$  and decrease of emission intensity. It can also be explained that, with increasing of EThN(CN)<sub>2</sub> loading from 23 wt% to the higher, as indicated by the fact that the pore size of wsg-EThN(CN)<sub>2</sub> showed no changes any more (Table 1), and EThN(CN)<sub>2</sub> may aggregate to a larger extent on the external surface of silica gel support, thus resulting in the remarkable decrease of its fluorescence emissions.

In order to explain the reasons for the stronger fluorescence emissions of dicyanamide based ILs confined in the mesoporous silica gel, the conformations of confined EMImN(CN)<sub>2</sub> and EThN(CN)<sub>2</sub> with varied IL loading were characterized by FT-Raman spectra, Fig. 5. As can be seen that, the symmetric stretching vibrational absorption band maximum of N=C ( $\nu_s$ ) was centered at 2194 cm<sup>-1</sup> observed for pure EMImN(CN)<sub>2</sub>. However, as for EMImN(CN)<sub>2</sub>-sg, with loading of 5 and 15 wt%,  $\nu_s$  of N=C was observed at 2205 and 2204 cm<sup>-1</sup> respectively, 10 cm<sup>-1</sup> higher than the absorption band observed in the spectra of pure EMImN(CN)<sub>2</sub>. While, with loading being increased to 47%,  $\nu_s$  shifted to 2196 cm<sup>-1</sup>, which was approaching the  $\nu_s$  of pure EMImN(CN)<sub>2</sub>. According to the pore sizes measurement of wsg-EMImN(CN)<sub>2</sub> discussed above, with EMImN(CN)<sub>2</sub> loading being increased from 15 wt% to the higher, the pore sizes of the silica gel were almost unvaried, and thus the increased IL inevitably more and more aggregated gradually tending to pure IL. Therefore,  $\nu_s$  of N=C showed a red shift with increasing of IL loading and  $\nu_s$  of N=C of EMImN(CN)<sub>2</sub>-sg with higher IL loadings was more close to the absorption band in the spectra of pure IL. The remarkable difference in the stretching vibrational spectra of N=C confined in the mesoporous silica gel in comparison with that in pure EMImN(CN)<sub>2</sub> may mean the conformational changes and realignment of N(CN)<sub>2</sub><sup>-</sup> anion in EMImN(CN)<sub>2</sub> after being confined. This can also be confirmed by the fact that, as shown in Fig. 5b, Raman absorption band of  $\nu_s$  (N=C) of EThN(CN)<sub>2</sub>-sg was observed at 2201 cm<sup>-1</sup> with 23 wt%, 9 cm<sup>-1</sup> higher than 2192 cm<sup>-1</sup> in the spectra of pure EThN(CN)<sub>2</sub>, and 2194 cm<sup>-1</sup> with 60 wt%, showing

a remarkable red shift correspondingly with  $\text{EThN}(\text{CN})_2$  loading being increased and a trend to the spectra of pure  $\text{EThN}(\text{CN})_2$  for  $\text{EThN}(\text{CN})_2$ -sg with higher IL loadings.

Although it is still not clear at this stage for the greatly enhanced fluorescence mechanism of the confined dicyanamide anion based ILs within mesoporous silica gel, it can be conjectured that, after being confined, the realignment of cation and anion of ILs may occur in comparison with pure ILs indicated by the vibrational changes in  $\text{N}\equiv\text{C}$  group as shown in the Raman spectra as well as the previous studies [21]. For the confined  $\text{EMImN}(\text{CN})_2$ , due to presence of  $\pi$  delocalized electrons in  $\text{N}(\text{CN})_2^-$ , stronger  $\pi$ - $\pi$  conjugated interactions between  $\text{N}(\text{CN})_2^-$  anions themselves may exist, giving enhanced fluorescence emission [34]. Furthermore, stronger  $\pi$  conjugated associations may also be formed between  $\text{N}(\text{CN})_2^-$  anion and  $\text{EMIm}$  cation, giving additional increasing in fluorescence emission. Therefore, the strongest enhanced emissions can be observed. For the confined  $\text{EThN}(\text{CN})_2$ , enhanced fluorescence emission may only be derived from  $\pi$ - $\pi$  conjugated interactions between  $\text{N}(\text{CN})_2^-$  anions due to the absence of  $\pi$  delocalized electrons over the cation. As to confined  $\text{EMImBF}_4$ , there only exists  $\pi$  stacking associations through surface overlapping of imidazolium ring in absence of  $\pi$ - $\pi$  conjugation of the anion of  $\text{BF}_4^-$ , thus the remarkably enhanced emission of  $\text{EMImBF}_4$ -sg cannot be observed.

Greatly enhanced fluorescence was firstly observed over the confined  $\text{EMImN}(\text{CN})_2$  and  $\text{EThN}(\text{CN})_2$  within mesoporous silica gel with 7–8 nm in pore sizes with  $\text{EMImN}(\text{CN})_2$  loading 15 wt% and  $\text{EThN}(\text{CN})_2$  loading 23 wt%. It can be expected that confined ILs within mesoporous matrices may also exhibit some other peculiar physicochemical properties in comparison with pure ILs, which are important for both understanding ILs themselves and potential application in catalysis, separation, solid electrolyte and luminescence material. The studies on this issue are ongoing.

#### 4. Conclusion

In this work,  $\text{EMImN}(\text{CN})_2$  and  $\text{EThN}(\text{CN})_2$  ILs which were physically confined into mesoporous silica gel were synthesized according to 'one pot' synthesis through a proper sol-gel method. After washing of ILs, silica gel was characterized to be mesoporous with pore sizes of 3–8 nm with varied IL loadings. Greatly enhanced fluorescence emissions of confined dicyanamide based ILs within mesoporous silica gel in comparison with pure ILs were exhibited, and furthermore, the fluorescence emissions were largely dependent on the IL loadings. Confined  $\text{EMImN}(\text{CN})_2$  with IL loading of 15 wt% within mesoporous silica gel with average pore diameter of 7–8 nm, and confined  $\text{EThN}(\text{CN})_2$  with IL loading of 23 wt% within mesoporous silica gel with average pore diameter of 6–7 nm gave the strongest emissions.

#### Acknowledgements

This work was financially supported by National Natural Science Foundation of China (Nos. 20533080 and 20503037).

#### Appendix A. Supplementary material

Supplementary data associated with this article can be found, in the online version, at doi:10.1016/j.cplett.2008.07.015.

#### References

- [1] D.M. Eigler, C.P. Lutz, W.E. Rudge, *Nature* 352 (1991) 600.
- [2] Y. Wada, *Surf. Sci.* 276 (1997) 386.
- [3] A.D. Mehta, M. Rief, J.A. Spudis, D.A. Smith, R.M. Simmons, *Science* 283 (1999) 1689.
- [4] M. Bruchez, M. Moronne, P. Gin, S. Weiss, A.P. Alivisatos, *Science* 281 (1998) 2013.
- [5] R. Bauer, G. Waldner, S. Fallmann, S. Hager, T. Krutzler, S. Malato, P. Maletzky, *Catal. Today* 53 (1999) 131.
- [6] S. Mitura, *Nanotechnology in Materials Science*, Elsevier, Amsterdam, 2000.
- [7] J. Jortner, *J. Phys. Chem.* 184 (1994) 283.
- [8] P. Alivisatos, *Science* 271 (1996) 933.
- [9] I. Last, J. Jortner, *Phys. Rev. Lett.* 87 (2001) 3401.
- [10] R. Kubo, *J. Phys. (Paris)* 38 (C2) (1977) 270.
- [11] M. Hartmann, A. Heidenreich, J. Pittner, V. Bonacic-Koutecky, J. Jortner, *J. Chem. Phys.* 102 (1998) 4069.
- [12] P.J. Thomas, G.U. Kulkarni, C.N.R. Rao, *Chem. Phys. Lett.* 321 (2000) 163.
- [13] C.N.R. Rao, B.C. Satishkumar, A. Govindaraj, M. Nath, *Chem. Phys. Chem.* 2 (2001) 78.
- [14] P. Avouris, P.G. Collins, *Science* 292 (2001) 706.
- [15] K.R. Seddon, *Nat. Mater.* 2 (2003) 363.
- [16] T. Welton, *Chem. Rev.* 99 (1999) 2071.
- [17] P. Wasserscheid, T. Welton, *Ionic Liquids in Synthesis*, Wiley-VCH, Weinheim, New York, 2003.
- [18] F. Shi, Y. Deng, *Spectrochim. Acta Part A* 62 (2005) 239.
- [19] M. Kanakubo, Y. Hiejima, K. Minami, T. Aizawa, H. Nanjo, *Chem. Commun.* (2006) 1828.
- [20] S. Chen, G. Wu, M. Sha, Sh Huang, *J. Am. Chem. Soc.* 129 (2007) 2139.
- [21] H. Park, Y. Choi, Y. Jung, W. Hong, *J. Am. Chem. Soc.* 130 (2008) 845.
- [22] A. Vioux, J. Le Bideau, M.-A. Neouze, F. Leroux, *Pat. Appl.* 2005/007746, WO 2857004, 2005.
- [23] M.-A. Neouze, J. Le Bideau, F. Leroux, A. Vioux, *Chem. Commun.* (2005) 1082.
- [24] M.-A. Neouze, J. Le Bideau, A. Vioux, *Prog. Solid State Chem.* 33 (2006) 217.
- [25] M.-A. Neouze, J. Le Bideau, P. Gaveau, S. Bellayer, A. Vioux, *Chem. Mater.* 18 (2006) 3931.
- [26] K. Lunstrout et al., *Chem. Mater.* 18 (2006) 5711.
- [27] J.L. Bideau, P. Gaveau, S. Bellayer, M.A. Néouze, A. Vioux, *Phys. Chem. Chem. Phys.* 9 (2007) 5419.
- [28] C. Pinilla, M.G. Del Pópulo, R.M. Lynden-Bell, J. Kohanoff, *J. Phys. Chem. B* 109 (2005) 17922.
- [29] D. Seth, A. Chakraborty, P. Setua, N. Sarkar, *J. Phys. Chem. B* 111 (2007) 4781.
- [30] A. Tesfai, B. El-Zahab, D.K. Bwambok, G.A. Baker, S.O. Fakayode, M. Lowry, I.M. Warner, *Nano. Lett.* 8 (3) (2008) 897.
- [31] A. Paul, P.K. Mandal, A. Samanta, *J. Phys. Chem. B* 109 (2005) 9148.
- [32] A. Paul, P.K. Mandal, A. Samanta, *Chem. Phys. Lett.* 402 (2005) 375.
- [33] A. Paul, P.K. Mandal, A. Samanta, *J. Chem. Sci.* 118 (2006) 335.
- [34] B. Valuer, *Molecular Fluorescence: Principles and Applications*, vol. 3, Wiley-VCH, 2001, pp. 56.